A&A 463, 1153–1163 (2007)
DOI: 10.1051/0004-6361:20066412

Astronomy & Astrophysics

Dual-line spectral and phase analysis of sunspot oscillations

K. Tziotziou[1], G. Tsiropoula[1], N. Mein[2], and P. Mein[2]

[1] National Observatory of Athens, Institute for Space Applications and Remote Sensing, 15236 Palea Penteli, Greece
e-mail: [kostas;georgia]@space.noa.gr
[2] Observatoire de Paris, Section de Meudon, LESIA, 92195 Meudon Principal Cedex, France
e-mail: [Nicole.Mein;Pierre.Mein]@obspm.fr

Received 18 September 2006 / Accepted 8 November 2006

ABSTRACT

Context. Sunspots exhibit a wide range of oscillatory phenomena within their umbrae and penumbrae.
Aims. We investigate the behavior of intensity and Doppler velocity oscillations in the umbra and the penumbra to study sunspot oscillations and their associations.
Methods. Simultaneous, high-cadence (8 s), two-dimensional, Ca II 8542 Å and Hα 6563 Å observations are used. Doppler velocity and intensity variations are studied with a wavelet spectral, phase difference and coherence analysis, both at distinct positions and within the whole umbra and the penumbra.
Results. The analysis reveals the presence of several umbral flashes (UFs) that seem to fill the whole umbra. The spectral analysis indicates oscillating elements of size 2.5″ to 5″ within the umbra with periods around the 3-min band and oscillation periods around the 5-min band within the penumbra. Two remarkable jumps of the oscillation period and the intensity-velocity phase difference are present at both umbra-penumbra and penumbra-superpenumbra boundaries reflecting a drastic change in physical and/or magnetic conditions. The intensity-velocity phase analysis shows a delay of the intensity response to the velocity variations in accordance with the physics of the observed sawtooth velocity behavior. Most of the UFs oscillate incoherently, while the calmest umbral area seems to be associated with velocity spreading from neighboring UFs. The derived incoherency among UFs in conjunction with the existence of coherently oscillating elements within the umbra suggests the presence of umbral areas with slightly different physical and/or magnetic field conditions.
Conclusions. The presented analysis provides further important constraints for realistic models and theoretical interpretations describing sunspot oscillations.

Key words. Sun: chromosphere – Sun: oscillations – Sun: sunspots

1. Introduction

Studies of oscillations and waves in the atmosphere of sunspots started since the detection of umbral flashes (UFs) in intensity images of the Ca H and K lines and the infrared triplet of Ca by Beckers & Tallant (1969). Intensity and/or velocity observations in various spectral lines revealed the existence of oscillations in the umbral photosphere (Bhatnagar et al. 1972) and chromosphere (Beckers & Schultz 1972; Giovanelli 1972) and of running penumbral (RP) waves (Zirin & Stein 1972; Giovanelli 1972).

Since then many observations have been performed of photospheric, chromospheric and transition region lines and increasing theoretical efforts have been undertaken to understand these periodic phenomena which contain crucial information regarding the dynamic structure of sunspots (see reviews by Lites 1992; Staude 1998; Bogdan 2000; Bogdan & Judge 2006). Such efforts include the study of photospheric magnetic field fluctuations in sunspots (Lites et al. 1998; Bellot Rubio et al. 2000). The derived observational characteristics of sunspot oscillations lead to the conclusion that these structures host a wide variety of waves and oscillatory phenomena. The power spectrum of umbral oscillations usually shows closely packed sharp peaks within the 5-min band at the photospheric level with an average rms velocity amplitude of 75 m s^{-1} (Lites 1992) and in the 3-min band at the chromospheric level (Brynildsen et al. 1999) however with larger rms velocity amplitudes; the latter can be as large as 8 km s^{-1}, as has been reported from observations in the Hα line by Tsiropoula et al. (2000). UFs appear as transient brightenings in parts of the umbra at chromospheric heights with periods of 2–3 min. UFs and umbral oscillations are probably different manifestations of the same phenomenon. The latter are present in almost every sunspot umbra, whereas UFs occur only locally and occasionally when the velocity amplitudes exceed a value, which, e.g. for the Ca II 8542 Å K line is ∼5 km s^{-1}, while in Hα are more rarely observed and perhaps only when the value of the velocity amplitude is large enough. RP waves have periods of 180–300 s and are easily detected in strong chromospheric resonance lines as disturbances propagating from the umbra-penumbra boundary out to the edge of the penumbra, becoming gradually invisible. UFs and RP waves are now believed to be either a) a visual pattern of later wavefront arrival of the same disturbance that creates UFs due to a longer travel path along divergent sunspot field lines or b) a physical, trans-sunspot wave traveling from the umbra outwards (see Tziotziou et al. 2006, hereafter Paper I).

The 5-min umbral oscillations are coherent over a large fraction of the umbral area (Abdelatif et al. 1986). On the other hand, as demonstrated by Lites (1986), the umbra at the chromospheric level does not oscillate as a whole, but rather the oscillations occur in small spatial regions within the umbra, the "oscillating elements", with sizes of 3″–4″ (see also Christopoulou et al. 2003) and velocity oscillation time series frequently exhibit a

"saw-tooth" behavior, i.e. a sharp shift from red to blue followed by a more gradual drift back to the red (see Paper I and references therein), indicating that significant wave steepening must be present.

Although the subject of several investigations, the nature of sunspot oscillations remains far from being settled. In this context simultaneous time-series observations of various spectral lines that sample the sunspot atmosphere at different heights can be useful in studying these periodic processes and giving clues about their nature. For instance, Giovanelli et al. (1978) found a phase lag between umbral oscillations observed in Fe I 5233 Å (photospheric) and Hα, indicating upward wave propagation. Gurman et al. (1982) observed oscillations in transition region lines and found an almost zero time lag between maximum blue shift and the intensity maximum indicative of upward propagating compressive waves. Uexküll et al. (1983), analysing time series of umbral oscillations in several photospheric and chromospheric lines, were able to show that chromospheric oscillations in sunspot umbrae are nearly standing, slightly upward propagating waves. Lites (1984, 1992) by measuring the phase differences of the oscillations in different spectral lines concluded that umbral oscillations in the chromosphere are upward-propagating compression waves (slow-mode waves) that develop shock fronts when they are sufficiently strong. The shock fronts is what we see as UF. Recently, Centeno et al. (2006) investigated the vertical propagation of slow magnetoacoustic waves and shock formation in a stratified magnetized sunspot atmosphere with radiative losses and found a good agreement between the theoretically computed time delay and that obtained from the cross-correlation of photospheric Si I 10827 Å and chromospheric He I 10830 Å velocity maps filtered around the 6 mHz band. As for the penumbral waves Sigwarth & Mattig (1997) by analysing oscillations at various atmospheric heights found upward propagating waves in the inner penumbra, and 5-min oscillations from the inner to the outer sunspot penumbra boundary and from the lower chromosphere to the temperature minimum, but not detectable below. In the upper chromosphere they found a significant change in the frequencies from the central penumbra (4 to 3 mHz) to the outer penumbra (2 mHz).

The aim of this work is to analyze high temporal and spatial resolution sunspot observations taken simultaneously in the Ca II 8542 Å and Hα lines. We investigate the behavior of intensity and Doppler shift oscillations in the umbra and the penumbra using a wavelet analysis and perform a phase and coherence analysis in order to provide further information on the subject of sunspot oscillations.

2. Observations

The sunspot under study (NOAA 9641, S13 W19) was observed on October 4th, 2001 with the Multichannel Subtractive Double Pass (MSDP) spectrograph (Mein 1991, 2002). The spectrograph is mounted on the German solar telescope VTT in Tenerife, Canary Islands and recorded a two-dimensional $183.5'' \times 19''$ band simultaneously in two lines, the Hα and the infrared Ca II 8542 Å from 09:53:39 to 10:10:51 UT with a cadence of 8 s and an estimated spatial resolution of $\sim 1''$. We refer the reader to Paper I for details concerning the observations and the reduction procedure. The result of the latter is 130 spatially co-aligned two-dimensional intensity and Doppler velocity images for each line, at ±0.29 Å and ±0.58 Å for Hα and at ±0.09 Å and ±0.135 Å for Ca II 8542 Å which were obtained with the bisector technique, as well as line-center intensity images in both lines. Positive Doppler shifts correspond to upward Doppler velocities and appear as bright in all presented velocity images.

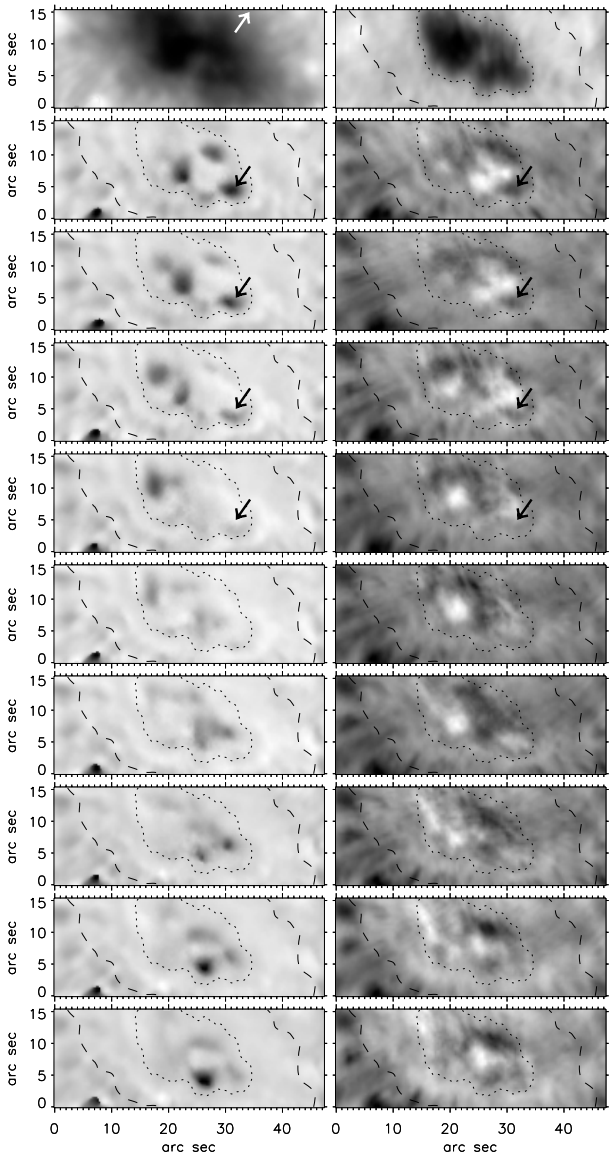

Fig. 1. *Top row*: A Ca II 8542 Å intensity image at ±0.135 Å (*left*) and an Hα intensity image at ±0.58 Å (*right*) of the observed sunspot. The dotted and dashed black contours denote respectively the approximate Hα umbra-penumbra and outer penumbra boundaries. North is towards the top of the panels, West is towards the left of the panels, while the white arrow in the left panel shows the direction to solar disc center. *Second to bottom row*: A sequence of Doppler velocity images in Ca II 8542 Å at ±0.135 Å (*left column*) and Hα at ±0.58 Å (*right column*) starting at 09:56:51 UT. Time runs from *top to bottom* and the cadence between consecutive images is 16 s. Black denotes downward Doppler velocities. The black arrow in the second to fifth row shows the UF discussed in 3.1 (see text).

In Fig. 1 (*top row*) we show an intensity image of the sunspot in Ca II 8542 Å at ±0.135 Å (*left panel*) and in Hα at ±0.58 Å (*right panel*). The sunspot was located within a region that gave a small number of C-class events the days prior to the observation. It is isolated and slightly elongated, while its penumbra unfortunately is not observed at the top of the image and it is partially observed at the bottom. The umbra looks bigger in the Ca II 8542 Å line than in Hα because of higher scattering

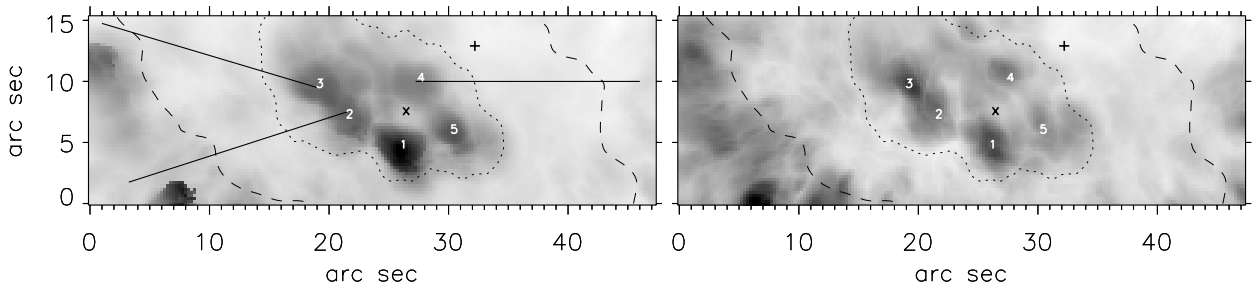

Fig. 2. The distribution of the highest amplitude downward Doppler velocity over the whole sequence per pixel of the observed field of view in Ca II 8542 Å at ±0.09 Å (*left panel*) and in Hα at ±0.29 Å (*right panel*). Black denotes highest downward velocities. White numbers indicate the five distinct UF positions while "×" marks the calmest umbral position (see text for details). The "+" marks the penumbral position used in the spectral analysis in 3.4 while the dotted and dashed black contours denote respectively the approximate Hα umbra-penumbra and outer penumbra boundaries. Overplotted lines in the left panel indicate the cuts used for the periodicity analysis shown in Fig. 6.

since the Ca II 8542 Å line is mainly sensitive to temperature, while Hα is mainly sensitive to density. The umbra-penumbra boundary is at ∼7−10″ from the sunspot center (dotted contour), while the penumbra-superpenumbra boundary (dashed contour) is about 10″ away from the umbra-penumbra boundary; both boundaries have been defined as the isocontours of specific values of Hα intensity and hence should be considered as approximate. A short light bridge appears to lie in the middle of the umbra indicating that the sunspot is splitting into two separate sunspots (observations from previous days show that the sunspot had a smaller and more compact umbra).

3. Results

In the following subsections we present the results of our analysis concerning UFs, RP waves, periodicities and phase differences.

3.1. Umbral flashes and RP waves

In Fig. 1 (*second to last row*) we present a sequence of nine Doppler velocity images in Ca II 8542 Å at ±0.135 Å (*left column*) and Hα at ±0.58 Å (*right column*) starting at 09:56:51 UT with a cadence of 16 s. UFs are visible in Hα as high upward or downward Doppler velocities within the sunspot, while in Ca II 8542 Å they only show up as high downward Doppler velocities (we will further discuss this in 3.2). They appear periodically at almost the same position in several distinct locations within the umbra. They either grow and diffuse at the same position or some of them (i.e. the one indicated with a black arrow in the second to fifth row of Fig. 1 which corresponds to flash No. 5 in Fig. 2) diffuse by slow spreading in their surrounding region.

In Fig. 2 we show the distribution of the highest amplitude downward Doppler velocity over the whole sequence at each pixel of the observed field of view in the Ca II 8542 Å line at ±0.09 Å (*left panel*) and in Hα at ±0.29 Å (*right panel*). Both spatial distributions are similar and show that UFs, associated with high amplitude downward Doppler velocities, appear at distinct locations within the umbra. We can clearly count at least five flashes in both images which are marked by white numbers. The UFs look quite extended and seem to fill almost the whole umbra, which could possibly be attributed to velocity spreading through well known umbral waves. There is only one small area within the umbra (marked by "×" in Fig. 2), around position $(x, y) = (26.5'', 7.5'')$, that shows the lowest amplitude downward velocities over time, defined hereafter as the "calmest umbral position".

RP waves seem to start at the umbra-penumbra boundary and are visible in both Ca II 8542 Å and Hα Doppler velocity images as propagating arcs in the penumbra (see Fig. 1). In our case, due to the limited field of view, they seem to have an azimuthal extent of at least ∼140° on the left side of the penumbra. In a previous paper we have discussed in detail the properties and propagation characteristics of these RP waves from the umbra to the outer penumbra (see Figs. 2 to 4 of Paper I and their description therein). We have shown that: a) most of the waves can be traced back inside the umbra (possible continuation of umbral waves), b) the propagation is smooth and continuous across the umbra-penumbra boundary, and c) their propagation speed decreases outwards.

3.2. Umbral Doppler velocities

As we have already mentioned, UFs show up as both high downward and upward Doppler velocities in Hα while in Ca II 8542 Å only as high downward Doppler velocities. This is because of both the intricate nature of the Ca II 8542 Å UF profile and the derivation of Doppler velocities with the bisector method. It is well known (e.g. Kneer et al. 1981; Uexküll et al. 1983, Tziotziou et al. 2002) that the Ca II 8542 Å line shows an emission on the blue side of its profile during UFs (e.g. see Fig. 1 in Tziotziou et al. 2002) which is usually interpreted in the literature as caused by the upward movement of hot material. A similar behavior has been demonstrated for example by Rutten & Uitenbroek (1991) in Ca II K-line profiles for an ad hoc shock travelling upwards in K_{2V} cell grains. The presence of this emission peak in the blue wing of the line will have as a result the derivation of downward Doppler velocities from the redshifted absorption core with the bisector method.

In Fig. 3 (*left panel*) we present an example of the Doppler velocity time evolution for a UF (No. 1 in Fig. 2) in Hα at ±0.29 Å (solid line) and in Ca II 8542 Å at ±0.09 Å (dotted line). The aforementioned effect of the Ca II 8542 Å flash profile in the determination of the corresponding Doppler velocities can be clearly seen since no upward Ca II 8542 Å Doppler velocities are derived. Both curves show a similar behavior. The downward (negative) Ca II 8542 Å UF Doppler velocities are of the order of 5 to 10 km s^{-1} and are larger than the respective Hα ones by a factor of 2 to 3, while the upward (positive) Hα Doppler velocities are of the same order as the Hα downward ones. The Hα Doppler velocity curve has a clear sawtooth

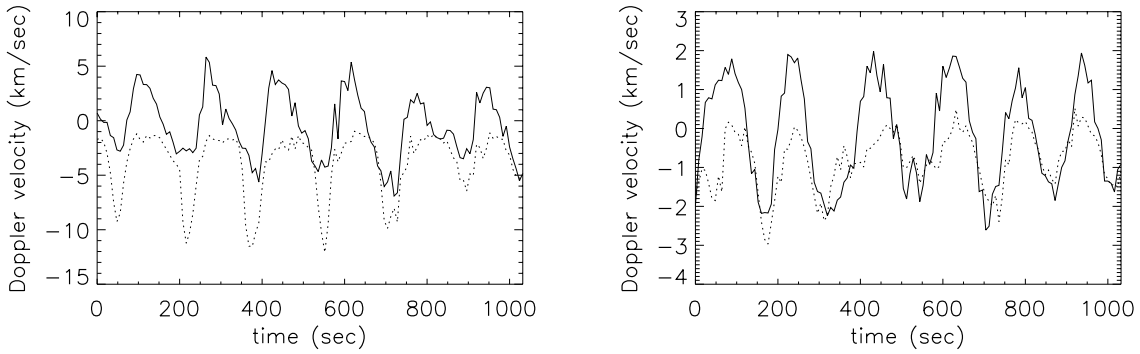

Fig. 3. Time evolution of the Doppler velocity for the UF No.1 of Fig. 2 (*left panel*) and for the calmest umbral position (*right panel*). Solid line represents the Hα Doppler velocity at ±0.29 Å, while dotted represents the Ca II 8542 Å Doppler velocity at ±0.09 Å. Positive Doppler velocities represent upward motion. We point out that the Doppler velocity scales of the two plots are different and that the calmest umbral position Doppler velocity amplitudes are smaller than the UF ones.

waveform which has already been observed and reported before (see reviews of Lites 1992; Bogdan & Judge 2006) and is suggestive of a shock behavior of the corresponding oscillation, consistent with the idea established in the literature about UFs. Rouppe van der Voort et al. (2003) and recently in a more detailed analysis Tziotziou et al. (2006) have shown that such a sawtooth behavior is seen also in the penumbra and sometimes as far as at the outer penumbra, which could provide important clues for the interpretation of the nature of UFs and RP waves.

In Fig. 3 (*right panel*) we show the Hα and Ca II 8542 Å Doppler velocity curves at ±0.29 Å and ±0.09 Å respectively for the calmest umbral position, defined in 3.1. Its Hα Doppler velocity curve shows a flash-like behavior, although much smoother than the flash Doppler velocity curve, with the upward Doppler velocity rise being either slightly faster or equally fast as its downward drift. The equivalent Doppler velocity amplitudes are lower than the flash Doppler velocity amplitudes (at least by a factor of two), but still much higher than the previously reported amplitudes for the quiet umbra (Tziotziou et al. 2002). It is not clear, from this figure, if this is an intrinsic oscillation or whether it is the result of velocity spreading (i.e. umbral waves) from the surrounding UF oscillations. We will further discuss this in 3.5.

3.3. Velocity-intensity relation in umbral flashes

As we have mentioned above the Hα Doppler velocity curve suggests a shock behavior in UFs. Unfortunately, there is no clear Hα Doppler velocity–intensity relation (see Fig. 4 top panel of the top right figure) due to the nature of the Hα wing formation which has intensity contributions from several atmospheric layers (a double-peaked contribution function for the Hα wing, see Leenaarts et al. 2006). However, this is not the case for the Ca II 8542 Å line. In Fig. 4 (top panel of the top left figure) we present the Doppler velocity curve (solid line) and the respective line wing intensity curve (dotted line) at ±0.09 Å in a UF. It can be clearly seen that whenever there is a high downward Doppler velocity in Ca II 8542 Å, which corresponds to a real downward velocity as the corresponding Hα curves in Fig. 3 suggest, there is a considerable increase of the Ca II 8542 Å intensity. The quick upward rise of the Hα velocity followed by a slow drift towards downward velocities is suggestive of a piston-like mechanism moving upwards into an area with a decreasing density with height. As a result its rise is quick until it reaches a boundary where it is quickly reflected downwards. Since this downward motion takes place into denser areas it is expected that it will be slower than its rise. One would also expect an increase in intensity emission during this downward motion, due to plasma compression, which will have a short delay compared to the velocity curve. Such a behavior is clearly seen in the corresponding Ca II 8542 Å intensity curves since the source function of the line is more sensible to collisions (i.e. the local temperature) and hence to compression. The intensity behavior for Hα (Fig. 4, top panel of top right figure) is more complicated due to the nature of this line, as we have mentioned above, and such a reaction to downward Doppler velocities is not clearly seen. We will further explore this in 3.4.2 with a phase difference analysis.

3.4. Spectral analysis and phase differences

For the study of sunspot oscillations we use a wavelet analysis (Torrence & Compo 1998) that permits not only the determination of any periodic signal, but also how this period varies with time. We refer the reader to Banerjee et al. (2001) and Tziotziou et al. (2004) for a detailed description of the wavelet analysis method, as well as for the methods used for determining the significance of the derived periods. To find the phase difference between two time series, a cross-wavelet transform is used (Tziotziou et al. 2005). We define also the coherence between two time series as the square of the cross-spectrum normalized by the individual spectra (Torrence & Compo 1998; Torrence & Webster 1999). This is a quantity between 0 and 1 measuring the cross-correlation between the two times series (the higher its value, the higher the correlation is).

3.4.1. Periodicities

In Fig. 4 we present the results of a wavelet spectral analysis at a position inside flash No.1 (*top row*), the calmest umbral position (*middle row*) and a penumbral position (*bottom row*) both for Doppler velocity and intensity variations in Ca II 8542 Å at ±0.09 Å (*left column*) and in Hα at ±0.29 Å (*right column*). The presented significance levels were determined by a comparison of the power spectrum to a background Poissonian noise spectrum. The randomization method described in Tziotziou et al. (2004) gives a) very high probabilities in the range of 95−100% (with a ±3.5% error for all probabilities reported hereafter) for the periods derived from both Ca II 8542 Å and Hα Doppler variations b) equally high probabilities (92−100%) for the derived periods from all Ca II 8542 Å intensity variations

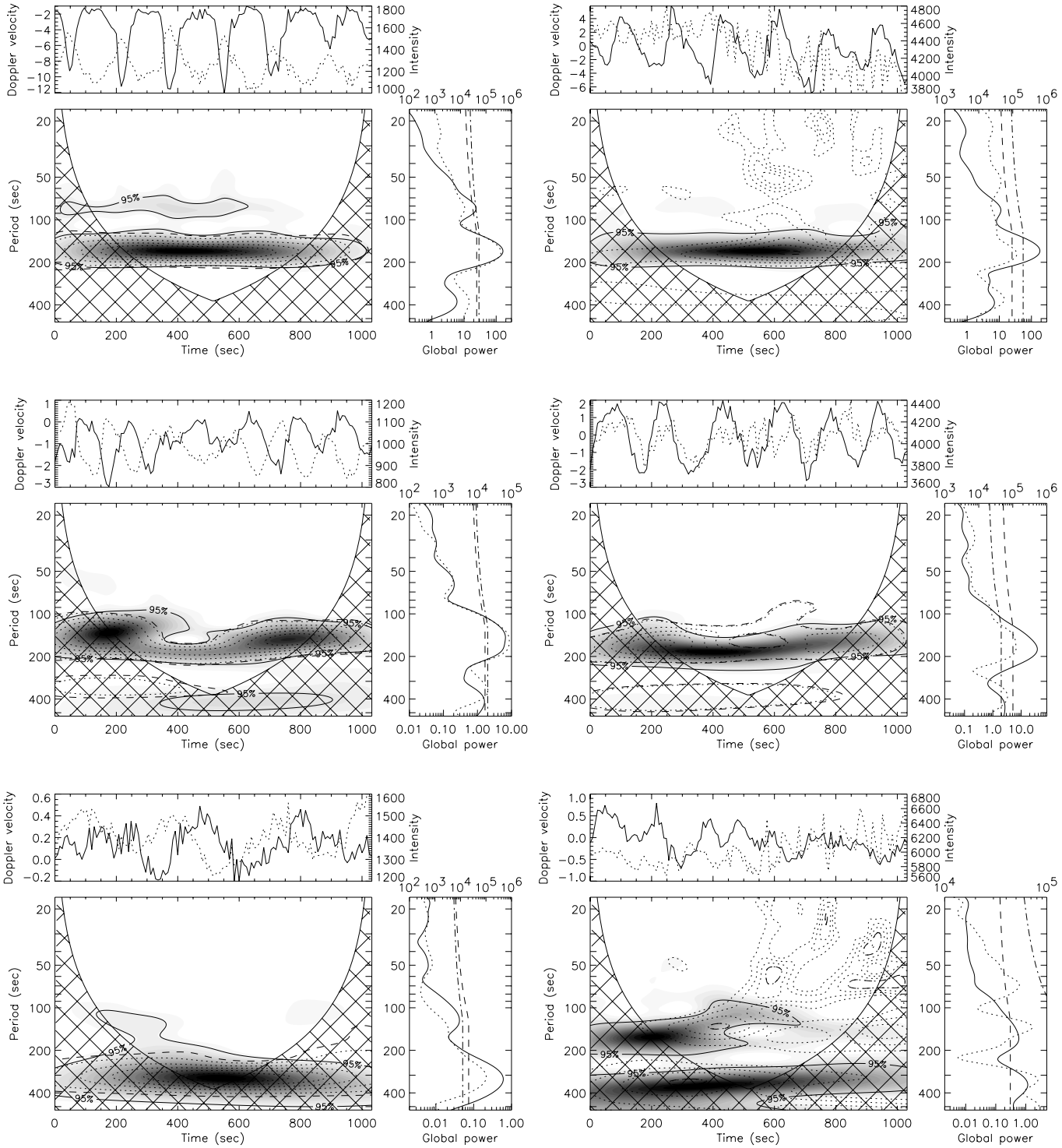

Fig. 4. Wavelet analysis at a) a position inside flash No. 1 of Fig. 2 (*top row*) b) the calmest umbral position marked with "×" in Fig. 2 (*middle row*) and c) a penumbral position marked with "+" in Fig. 2 (*bottom row*). Left column shows Ca II 8542 Å at ±0.09 Å, the right column shows Hα spectra at ±0.29 Å. In each figure the top panels show the time variations of the Doppler velocity in km s^{-1} (solid line, left ordinate) and intensity in counts (dotted line, right ordinate). The bottom left panels show the time-period calculated power spectra for the variations shown in the top panels. Filled contours correspond to Doppler velocity spectra with black representing high values of power (the solid contours represent the 95% significance level), dotted contours correspond to intensity spectra (the dashed contours show the 95% significance level). Cross-hatched regions indicate the regions where effects of zero padding of our finite time series may become important. The right panels show the global power spectrum, i.e. the average of the wavelet power spectrum over time of a) Doppler velocity (solid line, bottom abscissa) with the dashed line indicating the respective global significance level of 95% and b) intensity (dotted line, top abscissa) with the dotted-dashed line indicating the respective global significance level of 95%.

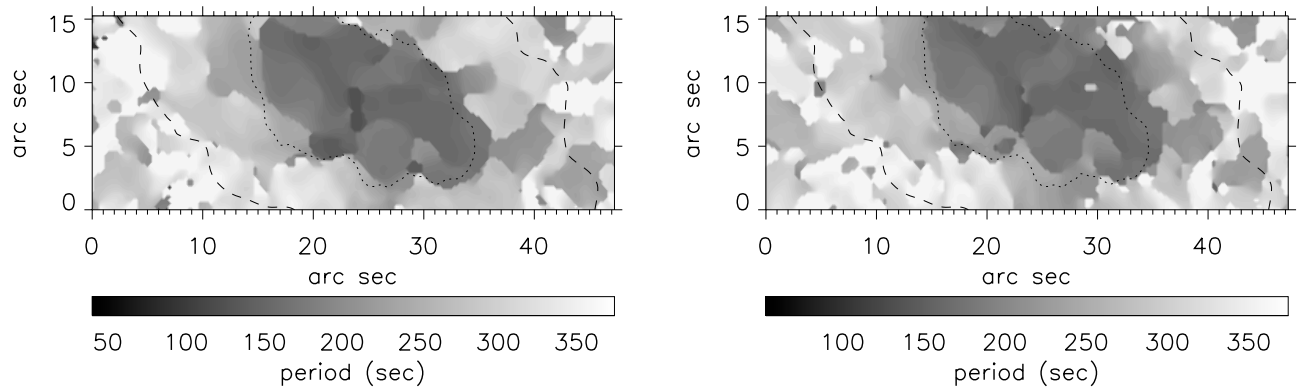

Fig. 5. Two-dimensional distribution of the period corresponding to the maximum of the global power spectrum obtained at each point with a wavelet analysis for the Ca II 8542 Å (*left panel*) and the Hα (*right panel*) Doppler velocity variations at ±0.09 Å and ±0.29 Å respectively. The dotted and dashed black contours denote respectively the approximate Hα umbra-penumbra and outer penumbra boundaries.

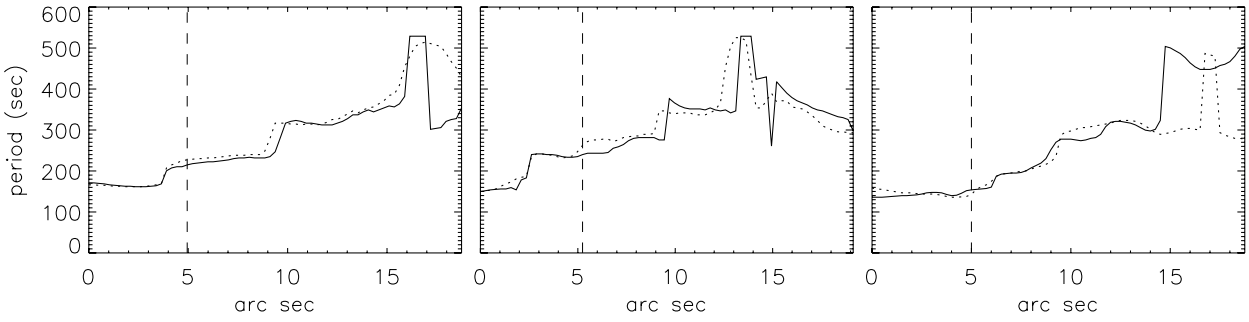

Fig. 6. Dominant period of oscillation along the top left cut (*left panel*) bottom left cut (*middle panel*) and horizontal right cut (*right panel*) of Fig. 2, calculated from the Hα Doppler velocity variations at ±0.29 Å (solid line) and the Ca II 8542 Å Doppler velocity variations at ±0.09 Å (dotted line). The vertical dashed lines indicate the approximate umbra-penumbra boundary. Length runs from the umbra (from UF positions 3, 2, and 4 respectively) towards the edge of the penumbra.

and the Hα intensity variations of the calmest umbral position and c) variable probabilities (0−80%) for the periods derived from Hα intensity variations in the flash position and the penumbral position. For the latter there are hardly any periods with significance levels above 95% in the respective spectra even from the comparison with a Poissonian noise distribution. For almost all positions, with the exception of the Hα spectra for the flash and the penumbra, both intensity and Doppler velocity power spectra and global power are strikingly similar. However, even for the two aforementioned exceptions the derived dominant periods are the same. The spectra show that a) the UF oscillates with periods around the 3-min band (160–180 s) b) the penumbra shows a dominant period around the 5-min band, the persistence of which over time indicates its physical importance although most of its power is found within the COI and hence maybe subject to edge-effects, and c) the calmest umbral position shows a similar spectral behavior as the UF position with periods around the 3-min band. The UF Ca II 8542 Å Doppler velocity power spectrum also shows a first harmonic around 90 s which is related to the fact that the Doppler velocity oscillation differs from a sinusoidal since the upward velocities are missing. However, obviously this is not the effect that gives a 180 s harmonic at the Hα power spectrum of the penumbral position.

In Fig. 5 we show a two-dimensional distribution of the period corresponding to the maximum of the global power spectrum obtained at each pixel of the image with a wavelet analysis for the Ca II 8542 Å (*left panel*) and the Hα (*right panel*) Doppler velocity variations at ±0.09 Å and ±0.29 Å respectively. The Ca II 8542 Å intensity variation distribution, which is not shown, is similar to the Doppler velocity distribution, while the Hα distribution is not regular due to the aforementioned behavior of the Hα line. Both distributions are qualitatively and quantitatively similar and they describe the occurrence distribution of the UFs. The whole umbra (even the calmest region) shows coherent oscillating elements of size 2.5 to 5″. It is interesting to note that more than one oscillating modes coexist within the umbra and the penumbra around the 3-min band and 5-min band respectively.

Both the umbra-penumbra and the penumbra-superpenumbra boundaries are distinguishable since there is a noticeable jump in the oscillation period at these boundaries (more obvious in the first one). This abrupt change, which could also be a very rapid but smooth transition that is not observed due to our spatial resolution, was reported in Paper I. The period behavior can be better seen in Fig. 6, where we present the variation of the dominant period of oscillation along the three cuts of Fig. 2, calculated from the Hα Doppler velocity variations at ±0.29 Å (solid line) and the Ca II 8542 Å Doppler velocity variations at ±0.09 Å (dotted line). We see that as we move from the umbra towards the penumbra the period rises slowly from the 3 min band to 5 min in the penumbra and even higher, close to 8 min further out. This increase is not absolutely smooth since there are several jumps observed. One of the first ones, close to the positions indicated with a dashed

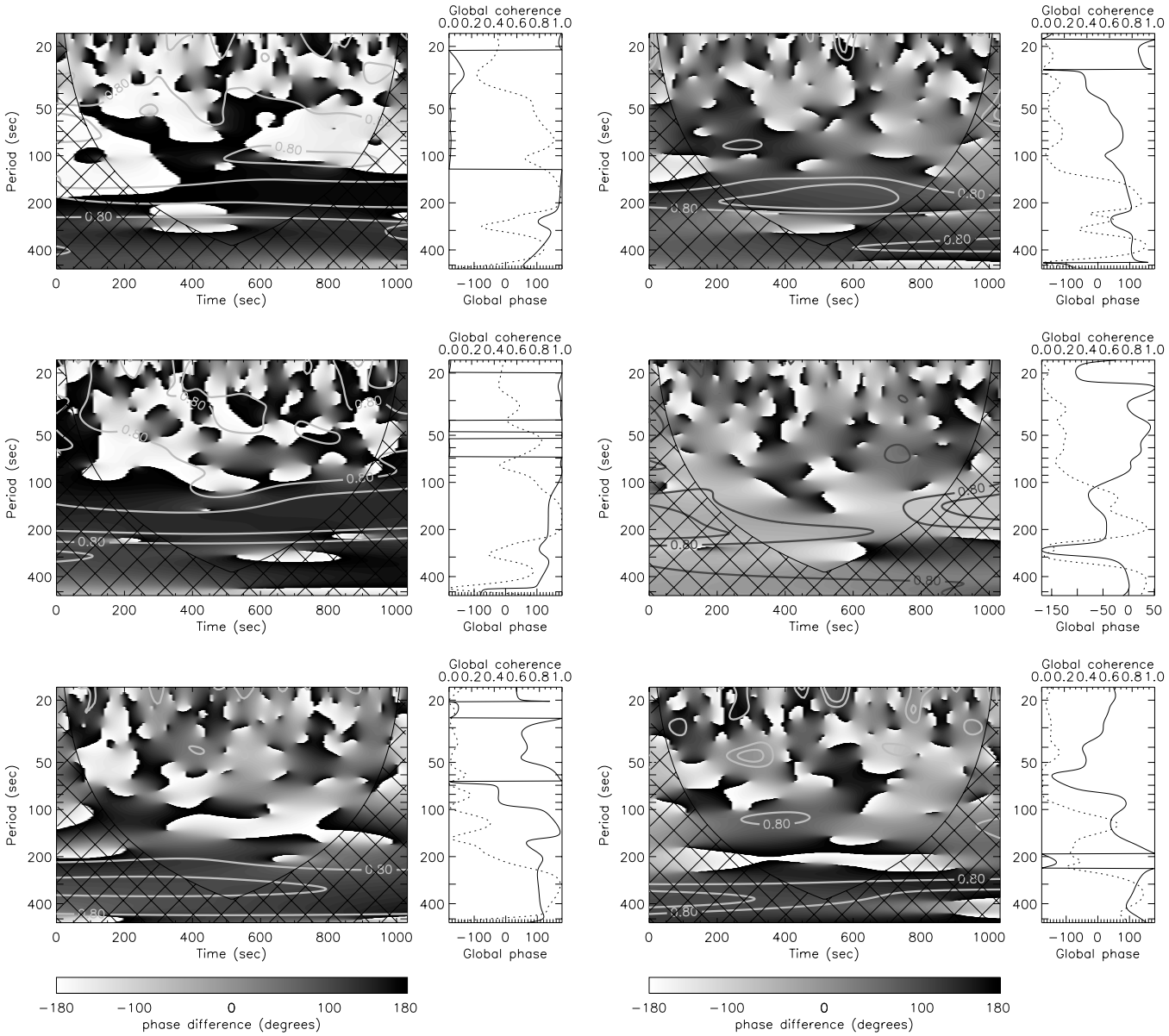

Fig. 7. Phase difference at the same a) flash position (*top row*) b) calmest umbral position (*middle row*) and c) penumbral position (*bottom row*) of Fig. 4 between the Doppler velocity and intensity variations presented at the respective top panels of that figure. The Doppler velocity curve is taken as the reference curve. Left column shows Ca II 8542 Å, while right column shows Hα phase differences. In each figure the left panels show the time-period calculated phase differences. Overplotted contours show the calculated coherence levels of 0.8 and higher (non-labelled contours correspond to a higher coherence). Cross-hatched regions indicate the regions where effects of zero padding of our finite time series may become important. The right panels show the global phase difference, i.e. the average of the phase difference over time (solid line, bottom abscissa) and the equivalent global coherence (dotted line, top abscissa).

line, is probably associated with the umbra-penumbra boundary indicating a drastic change in the local physical conditions, for example density and/or magnetic field. A second jump around position 10″ (less clear for the third cut), in the penumbra, could be associated with a difference in the structure of magnetic fields from the middle of the penumbra outwards as suggested by Del Toro Iniesta (2001) and reported in Tziotziou et al. (2002). The third jump to very high periods could be associated with the penumbra-superpenumbra boundary since high periods of the order of 10 min have been reported for the superpenumbra (Christopoulou et al. 2000)

It seems that in all cases the behavior of the period from the umbra across the penumbra to the superpenumbra is dictated by drastic changes of the local physical conditions and most probably changes of the magnetic field line inclination as suggested in Paper I.

3.4.2. Doppler velocity-intensity phase differences

In Fig. 7 we show the phase difference between the Doppler velocity curves and the respective intensity curves presented in Fig. 4 (top panels of individual figures) for the same flash position (*top row*), calmest umbral position (*middle row*) and penumbral position (*bottom row*). The Doppler velocity curve is taken as the reference curve. Overplotted contours indicate the calculated coherence levels of 0.8 and higher. The global phase

difference is the time average of the phase difference with cross-power weighting as defined in Tziotziou et al. (2005), while global coherence is the equivalent time average of the calculated coherence. We see that:

- For the UF and the penumbral position the Ca II 8542 Å and Hα phase difference behavior is qualitatively the same where coherence takes high values, mostly around the 3-min band for the UF position and around the 5-min band for the penumbral position.
- Quantitatively for these two positions – around the corresponding most dominant period – we obtain a) 174 and 94 degrees for the Ca II 8542 Å and Hα UF global phase difference respectively, and b) 104 and 111 degrees for the Ca II 8542 Å and Hα penumbra global phase difference respectively. The respective values differ (especially for the UF) as a result of the intricate nature of the Ca II 8542 Å Doppler velocity flash profile and/or the differences in the formation of these lines which is reflected in the intensity profiles. For both positions the global phase difference is positive meaning that there is a delay in the reaction of intensity to the respective velocity variation (even if this is not clearly visible in the corresponding Hα curves), as suggested from the shock shape of the Hα Doppler velocity curve in 3.2 and explained therein. It also implies an association of UFs and RP waves suggesting that either both phenomena share a common driver or that RP waves are driven by UFs.
- For the calmest umbral position the Ca II 8542 Å and Hα phase differences seem to have opposite signs where the coherence takes high values around the 3-min band. Moreover, the Ca II 8542 Å and Hα global phase differences are 137 and −43 degrees respectively which are 180 degrees apart. This probably suggests that the nature of this area is different from the UF areas.

Figure 8 shows the two-dimensional distribution of the global phase difference which corresponds to the global coherence (and power spectrum) maximum between the Ca II 8542 Å Doppler velocity and intensity variations at ±0.09 Å at each pixel of the image, with the Doppler velocity curve taken as the reference curve. The corresponding Hα distribution is not as smooth as the Ca II one, due to the formation properties of the Hα line and the absence of a clear relation between velocity and intensity, and hence is not presented. We see that the dominant phase difference is positive for both the umbra and the penumbra with highest values (more than 130°) within the umbra. There is only an area around the lower left part of the umbra which shows strong negative phase difference (∼−180°); this is an artifact due to the wraparound effect, when angle values just above π are transformed into values just below $-\pi$ (or vice versa). The positive phase difference means that there is a delay in the reaction of intensity to the respective velocity variation in accordance with the existence of shock-shaped Doppler velocity profiles in the umbra and the penumbra (see Paper I) and the discussion in 3.2. The smaller phase differences in the penumbra compared to the ones in the umbra could reflect an increase in the density which would lead to faster compression, a mechanism that could equally work for both the visual pattern and the trans-sunspot wave scenario reported for penumbral waves (see Paper I). There are two remarkable features in this two-dimensional distribution, two sharp decreases of the dominant phase difference at the umbra-penumbra boundary and close to the penumbra-superpenumbra boundary. This is similar to the respective two-dimensional period distribution behavior shown in Fig. 5 (*left panel*) and may reflect drastic changes of the local physical (i.e. density and/or magnetic) conditions.

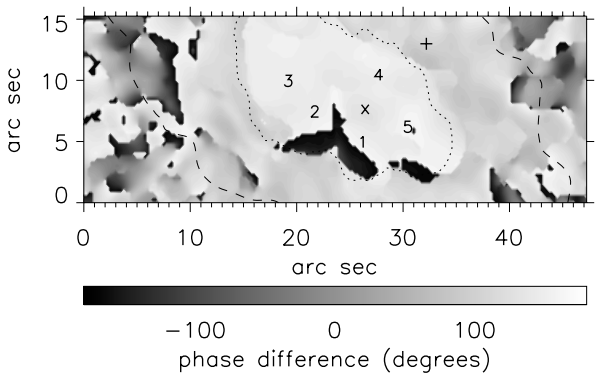

Fig. 8. Two-dimensional distribution of the global phase difference corresponding to the global coherence (and power spectrum) maximum between the Ca II 8542 Å Doppler velocity and intensity variations at ±0.09 Å. The Doppler velocity curve is taken as the reference curve. Numbers indicate the five distinct UF positions while "×" and "+" mark respectively the calmest umbral position and the penumbral position used in our analysis. The dotted and dashed black contours denote respectively the approximate Hα umbra-penumbra and outer penumbra boundaries.

3.4.3. Two-dimensional phase difference distribution between Doppler velocity variations

A preliminary investigation of the phase difference between Ca II 8542 Å Doppler velocity variations at ±0.09 Å and ±0.135 Å (which has a less complicated formation than Hα) revealed very small phase differences that could be due to errors, and thus hard to interpret. The interpretation of the phase difference between velocity variations at different wavelength positions of the same line profile would be rather difficult without detailed radiative transfer calculations of the formation of the line within the sunspot atmosphere.

When looking at the UF Doppler velocity variations presented in Fig. 3 (*left panel*) the rise of the Ca II 8542 Å Doppler velocity seems to start before the corresponding Hα Doppler velocity rise while the decrease of the Hα Doppler velocity starts before the Ca II 8542 Å one. This clearly points to a piston-like mechanism for the UFs and leads us to investigate the phase difference between the Doppler velocity curves of the two lines. Figure 9 shows the two-dimensional distribution of the global phase difference corresponding to the global coherence (and power spectrum) maximum between the Ca II 8542 Å Doppler velocity variations at ±0.09 Å and the Hα Doppler velocity variations at ±0.29 Å, with the Ca II 8542 Å Doppler velocity curve taken as the reference curve. The global phase difference is positive (∼50°) within the umbra while in the penumbra is either positive (but with lower values) or close to zero, again indicating different physical conditions in these two sunspot areas. One cannot say with certainty if the Ca II 8542 Å Doppler velocity variations at ±0.09 Å originate from a lower atmospheric level than the Hα Doppler variations at ±0.29 Å without precise calculations of the formation heights of these lines within the sunspot and its vicinity. However, taking into account that this study, as well as previous ones, suggest upward motions within the umbra, we conclude that the Ca II 8542 Å Doppler variations come from a deeper layer. We note that: a) the umbra-penumbra

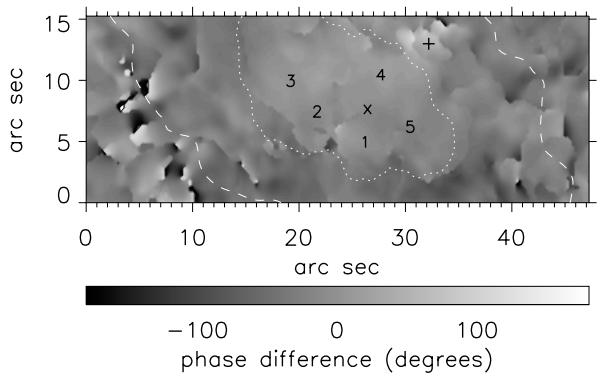

Fig. 9. Two-dimensional distribution of the global phase difference corresponding to the global coherence (and power spectrum) maximum between the Ca II 8542 Å Doppler velocity variations at ±0.09 Å and the Hα Doppler velocity variations at ±0.29 Å. The Ca II 8542 Å Doppler velocity curve is taken as the reference curve. Numbers indicate the five distinct UF positions while "×" and "+" mark respectively the calmest umbral and penumbral position used in our analysis. The dotted and dashed white contours denote respectively the approximate Hα umbra-penumbra and outer penumbra boundaries.

boundary and the outer border of the penumbra are again clearly visible and b) the behavior of the two lines is different in the sunspot and its vicinity, most probably due to temperature effects.

3.4.4. Phase difference between different umbral positions

As we have mentioned in 3.1 there are at least five distinct UFs present in the sunspot umbra (see also Fig. 2). Figure 10 shows the phase difference, both in Ca II 8542 Å (*left panel*) and Hα (*right panel*), obtained from Doppler velocity variations (at ±0.135 Å and ±0.58 Å respectively) of the four flash positions and the calmest umbra position with the fifth flash velocity curve (No. 1 in Fig. 2) used as a reference. The phase difference behavior is strikingly similar (except for UF No. 5), both qualitatively and quantitatively, for both lines within the 3-min band (shaded area) which is the dominant oscillation period. This similarity again stresses the fact that despite the intricate nature of the Ca II 8542 Å flash line profile, the resulting Doppler velocity curve registers the signature of the UF mechanism as accurately as the Hα Doppler velocity curve. The different behavior of UF No. 5 probably rises from the fact that this flash appears too weak in Hα (see Fig. 2) and hence will not be further considered.

We see from the derived phase difference values (around the 3-min band) that three out of five UFs and the calmest umbral point are not in phase. Only flashes No. 2 and 3 seem probably to be almost in phase, flash No. 1 appears after all other flashes and the calmest umbral position is the only one with a positive phase difference, suggesting that it appears well after all flashes; this will be further discussed in 3.5.

The fact that some flashes are not in phase could be interpreted either as due to a) different pistons independently acting in the umbra, or b) different reactions of different parts of the umbra to a single piston due to local physical differences (i.e. different magnetic field topology). However, it is impossible to deduce from these observations which of the two suggestions is valid.

3.5. Nature of the calmest umbral position

As we have discussed in 3.2 (see Fig. 3) the calmest umbral position shows a similar Doppler velocity behavior to UFs, although with lower velocity amplitudes. Furthermore, the periodicity analysis in 3.4.1 shows that both the UFs and the calmest umbral position oscillate with similar periods. So, what is the real nature of the calmest umbral position? Are the Doppler velocity and periodicity behavior the result of a) an intrinsic piston-like oscillation similar to UFs working in different physical conditions or b) umbral wave spreading from the surrounding UF oscillations? There are a number of clues that point to the latter suggestion:

- The smoother Doppler velocity behavior (Fig. 3, *right panel*) looks like that of penumbral waves (see Paper I) and is more suggestive of a smooth oscillation or a wave rather than a piston-like mechanism. Furthermore, its Ca II 8542 Å oscillations are closer to a sinusoidal than the corresponding UF ones which is also reflected to the absence of the 90 s harmonic (see top and middle left power spectrum panels of Fig. 4).
- The Doppler velocity amplitude and periodicity seem to be similar to that of running umbral waves (Kobanov & Makarchik 2004).
- The Doppler velocity-intensity relationship (Fig. 4, top panel of the middle right figure). Although no clear relationship exists for UFs (as Fig. 4 top panel of the top right figure shows) – which are more likely due, as we have explained, to a piston-like mechanism – there is clearly a relationship present for the calmest umbral position; its Hα intensity oscillations are more discernible which is also reflected in a higher corresponding global significance for the most dominant period. Such a relationship, although less clear for the last part of the time sequence, is present also for the penumbral position (Fig. 4, top panel of the bottom right figure) which is associated with running waves (in this case penumbral waves). Hence the calmest umbral position behavior seems to be associated with waves rather than a piston-like mechanism. This is furthermore supported by the phase difference analysis between the Doppler velocity curve and the intensity curve, presented in 3.4.2, which suggests that the nature of UFs and the calmest umbral area is different.
- As shown in 3.4.4 the velocity curve of the calmest umbral position has a positive phase difference with respect to UFs suggesting that it appears well after them and thus it could be due to velocity spreading (wave) caused by the UFs. Furthermore, the closer UFs (e.g. UF No. 1) have a smaller phase difference with the calmest umbra point than the further ones (e.g. No. 3) suggesting that the calmest umbral point experiences the effects of UFs after propagation. A calculated propagation velocity of ∼35−40 km s^{-1} from the relative phase differences is in accordance with previous studies (Kobanov & Makarchik 2004; Tsiropoula et al. 2000).

Hence the calmest umbral position behavior seems to be associated with velocity spreading from neighboring flash positions via running umbral waves rather than a piston-like mechanism.

4. Discussion and conclusions

The properties and behavior of sunspot oscillations have been investigated using high temporal cadence Ca II 8542 Å and

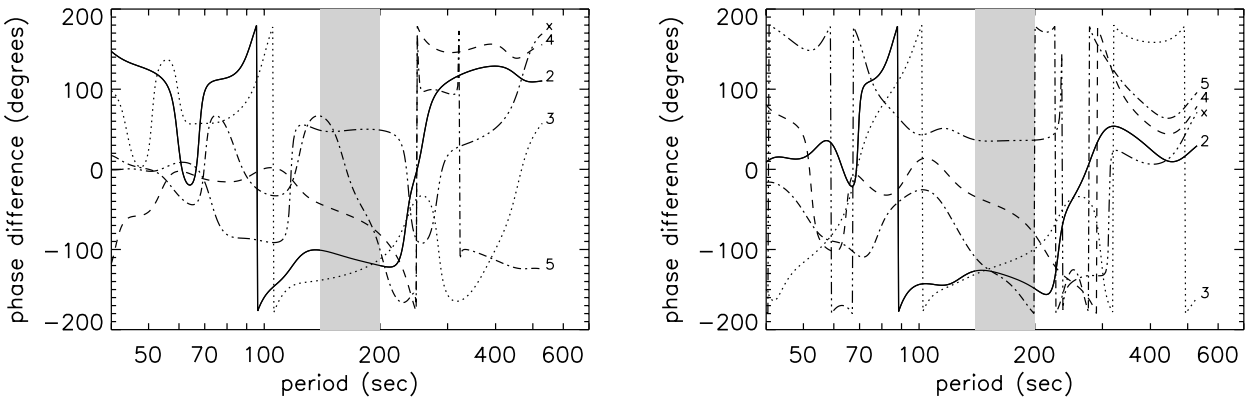

Fig. 10. Phase difference in Ca II 8542 Å (*left panel*) and Hα (*right panel*), obtained from Doppler velocity variations (at ±0.135 Å and ±0.58 Å respectively), for four flash positions and the calmest umbral position with the fifth flash velocity curve (No. 1 in Fig. 2) used as a reference. The phase difference curves are marked with the corresponding numbers and signs shown in Fig. 2 and the shaded area shows the 3-min band which corresponds to the dominant oscillation period.

Hα MSDP observations. The analysis has revealed a large number of extended UFs that fill almost the whole umbra of the sunspot, except a very small area, and RP waves propagating from the umbra-penumbra boundary towards the outer penumbra. The observational characteristics of both oscillatory phenomena and their possible association have been extensively analyzed in Paper I.

The umbral Doppler velocity curves have a clear sawtooth waveform suggestive of a piston-like mechanism for the respective oscillations. The velocity-intensity relation and the apparent time delay of the intensity compared to the velocity variation reveals that the intensity increase is due to plasma compression during the descending phase of the sawtooth velocity profile.

The spectral analysis at individual positions, as well as two-dimensional period distributions on the sunspot area, indicate that more than one oscillating modes coexist around the 3-min band within the umbra and around the 5-min band in the penumbra. The two-dimensional period maps also reveal several coherent oscillating elements with sizes of 2.5 to 5″ within the umbra which describe the spatial occurrence distribution of the UFs. If UFs do share a common extended source below the visible photosphere, as suggested by Rouppe van der Voort et al. (2003) and more recently by Bogdan & Judge (2006), and represent upward propagating wavefronts along magnetic field lines, as initially suggested by López Ariste et al. (2001) from an analysis of the linear polarization of the Ca II infrared triplet lines, then the existence of such elements would suggest the presence of similar size areas with coherent but slightly different physical conditions or magnetic field inclinations.

A remarkable finding of this work is a noticeable jump in the oscillation period at the umbra-penumbra boundary and less clearly in the penumbra-superpenumbra boundary which indicates drastic changes of the local physical conditions and/or the magnetic field topology and has been discussed extensively in Paper I in association with the propagation of RP waves. Both jumps are even more noticeable in the two-dimensional maps of the phase difference between velocity and intensity variations. The positive time delay of the intensity variations compared to the respective velocity variations within the umbra and the penumbra is in accordance with the existence of sawtooth profiles observed as far as at the outer penumbra (reported in Paper I), while the decrease of that time delay as we move from the umbra outwards would indicate in such a scenario an increase of the corresponding density that would lead to a faster reaction of the plasma during the descending velocity phase of the sawtooth profile.

Concerning the association of UFs and RP waves and more specifically the question of whether the latter are a visual pattern created by a common source with UFs or a trans-sunspot wave driven by UFs, the presented spectral and phase analysis does not provide any direct arguments supporting one scenario over the other since most of the derived results can be explained by both mechanisms.

In both two-dimensional period and phase difference maps presented in this analysis there is no fibril-like structure present in the penumbra. This is most probably the result of spatial resolution, and not an indication that RP waves are not directly associated with the fibril structure observed around sunspot umbrae.

Three out of five UFs seem not to be in phase with each other. If they indeed share a common source below the visible photosphere, this different non-coherent reaction would suggest different physical and/or magnetic field conditions existing within the umbra in accordance with the aforementioned observation of existing oscillating elements with a 2.5 to 5″ size. However, the possibility of several different piston-like sources would not be excluded by the current analysis.

As we have mentioned before there is a small area within the umbra, called the calmest umbral position, that does not show a UF but its velocity curve has similar characteristics to a UF velocity curve. Its smoother velocity behavior, the velocity amplitude and periodicity similar to umbral waves, its Doppler velocity-intensity relationship and the positive time delay with respect to UFs seem to indicate that this area is associated with velocity spreading – via running waves – from the neighboring flashes.

This study reveals new important findings concerning the different oscillation modes present both in the umbra and the penumbra, their behavior and possible association and provides further constraints for future realistic models and theoretical interpretations of sunspot oscillations.

Acknowledgements. The VTT telescope is operated on the island of Tenerife by the Kiepenheuer Insitute in the Spanish Observatorio del Teide of the Instituto de Astrofísica de Canarias. We thank A. Anastasiadis for constructive discussions and comments. K.T. acknowledges support by Marie Curie European Reintegration Grant MERG-CT-2004-021626.

References

Abdelatif, T. E., Lites, B. W., & Thomas, J. H. 1986, ApJ, 311, 1015
Banerjee, D., O'Shea, E., Doyle, J. G., & Goossens, M. 2001, A&A, 371, 1137
Beckers, J. M., & Schultz, R. B. 1972, Sol. Phys., 27, 61
Beckers, J. M., & Tallant, P. E. 1969, Sol. Phys., 7, 351
Bellot Rubio, L. R., Collados, M., Ruiz Cobo, B., & Rodríguez Hidalgo, I. 2000, ApJ, 534, 989
Bhatnagar, A., Livingston, W. C., & Harvey, J. W. 1972, Sol. Phys., 27, 80
Bogdan, T. J. 2000, Sol. Phys., 192, 373
Bogdan, T. J., & Judge, P. G. 2006, Phil. Trans. R. Soc. A, 364, 313
Brynildsen, N., Maltby, P., Leifsen, T., Kjeldseth-Moe, O., & Wilhelm, K. 1999, Sol. Phys., 191, 129
Centeno, R., Collados, M., & Trujillo Bueno, J. 2006, ApJ, 640, 1153
Christopoulou, Georgakilas, A. A., & Koutchmy, S. 2000, A&A, 354, 305
Christopoulou, E. B., Skodras, A., Georgakilas, A. A., & Koutchmy, S. 2003, ApJ, 591, 416
del Toro Iniesta, J. C. 2001, in ASP Conf. Ser., Magnetic fields across the Hertzprung-Russell diagram, ed. G. Mathys, & S. K. Solanki, 248, 35
Giovanelli, R. G. 1972, Sol. Phys., 27, 71
Giovanelli, R. G., Harvey, J. W., & Livingston, W. C. 1978, Sol. Phys., 58, 347
Gurman, J. B., Leibacher, J. W., Shine, R. A., Woodgate, B. E., & Henze, W. 1982, ApJ, 253, 939
Kneer, F., Mattig, W., & Uexküll, M. v. 1981, A&A, 102, 147
Kobanov, N. I., & Makarchik, D. V. 2000, A&A, 424, 671
Leenaarts, J., Rutten, R. J., Sütterlin, P., Carlsson, M., & Uitenbroek, H. 2006, A&A, 449, 1209
Lites, B. W. 1984, ApJ, 277, 874
Lites, B. W. 1986, ApJ, 301, 992
Lites, B. W. 1992, in NATO ASIC Proc., Sunspots: Theory and Observations, ed. J. H. Thomas, & N. O. Weiss (Dordrecht: Kluwer Academic), 375, 261
Lites, B. W., Thomas, J. H., Bogdan, T. J., & Cally, P. S. 1998, ApJ, 497, 464
López Ariste, A., Socas-Navarro, H., & Molodij, G. 2001, ApJ, 552, 871
Mein, P. 1991, A&A, 248, 669
Mein, P. 2002, A&A, 381, 271
Rouppe van der Voort, L. H. M., Rutten, R. J., Sütterlin, P., Sloover, P. J., & Krijger, J. M. 2003, A&A, 403, 277
Rutten, R. J., & Uitenbroek, H. 1991, Sol. Phys., 134, 15
Sigwarth, M., & Mattig, W. 1997, A&A, 324, 743
Staude, J. 1998, in Third Advances in Solar Physics Euroconference: magnetic fields and oscillations, ed. B. Schmieder, A. Hofmann, & J. Staude, ASP Conf. Ser., 184, 113
Torrence, C., & Compo, G. P. 1998, Bull. Amer. Meteor. Soc., 79, 61
Torrence, C., & Webster, P. J. 1999, J.Climate, 12, 2679
Tsiropoula, G., Alissandrakis, C. E., & Mein, P. 2000, A&A, 355, 375
Tziotziou, K., Tsiropoula, G., & Mein, P. 2002, A&A, 381, 279
Tziotziou, K., Tsiropoula, G., & Mein, P., 2004, A&A, 423, 1133
Tziotziou, K., Tsiropoula, G., & Sütterlin, P. 2005, A&A, 444, 265
Tziotziou, K., Tsiropoula, G., Mein, N., & Mein, P. 2006, A&A, 456, 689 (Paper I)
Uexküll, M. v., Kneer, F., & Mattig, W. 1983, A&A, 123, 263
Zirin, H., & Stein, A. 1972, ApJ, 178, L85